Journal of Power Sources 247 (2014) 729–737

Contents lists available at ScienceDirect

Journal of Power Sources

journal homepage: www.elsevier.com/locate/jpowsour

Extraction of battery parameters of the equivalent circuit model using a multi-objective genetic algorithm

Jonathan Brand, Zheming Zhang, Ramesh K. Agarwal*

Department of Mechanical Engineering & Materials Science, Washington University in St. Louis, USA

HIGHLIGHTS

- A simple but accurate battery model based on equivalent-circuit is required.
- Multi-objective genetic algorithm is utilized for extracting performance parameters.
- Battery performance is accurately predicted once parameters are optimally extracted.
- The parameter-extracting code is widely applicable for various types of batteries.
- It can serve as a robust and reliable tool for extracting the battery parameters.

ARTICLE INFO

Article history:
Received 26 June 2013
Received in revised form
1 September 2013
Accepted 3 September 2013
Available online 11 September 2013

Keywords:
Battery performance
Equivalent circuit model
Multi-objective genetic algorithm
Parameter extraction

ABSTRACT

A simple but reasonably accurate battery model is required for simulating the performance of electrical systems that employ a battery for example an electric vehicle, as well as for investigating their potential as an energy storage device. In this paper, a relatively simple equivalent circuit based model is employed for modeling the performance of a battery. A computer code utilizing a multi-objective genetic algorithm is developed for the purpose of extracting the battery performance parameters. The code is applied to several existing industrial batteries as well as to two recently proposed high performance batteries which are currently in early research and development stage. The results demonstrate that with the optimally extracted performance parameters, the equivalent circuit based battery model can accurately predict the performance of various batteries of different sizes, capacities, and materials. Several test cases demonstrate that the multi-objective genetic algorithm can serve as a robust and reliable tool for extracting the battery performance parameters.

1. Introduction

In recent years, there has been tremendous emphasis as well as effort devoted towards the development of high performance batteries mainly driven by their need as a power source for an electric or hybrid electric vehicle [1] and as an energy storage device for intermittent energy supply sources such as solar and wind [2]. Rechargeable batteries are particularly suitable for these applications because of their potential for high round-trip efficiency, long operating life and scalability [3]. In addition to these technical requirements, the battery should be of low enough cost to be cost effective as a power source for an electric vehicle or as an energy storage device.

To study the behavior of electric vehicles, manufacturers model the electric drive train. In order to do so, the energy source of these drive trains, the battery, needs to be accurately modeled as well. There are essentially four types of battery models that are used to model its performance; these can be categorized as the experimental models, the electrochemical models, the mathematical models and the electric circuit based models. The experimental and electrochemical models are not well suited to model the cell dynamics; hence they cannot be used reliably to determine the State-of-Charge (SOC) of the battery [4]. Furthermore, the electrochemical models are computationally expensive and require extensive experimentation for determining the parameters of the model [1]. The mathematical models of the batteries are based on stochastic approaches or empirical equations to predict the run time, capacity and efficiency of the batteries [1]. Furthermore, the mathematical models do not have direct relation between the battery model parameters and the I–V (current–voltage) characteristics of the batteries; hence they have limited use in circuit simulations.

* Corresponding author. 1 Brookings Drive, St. Louis, MO 63130, USA. Tel.: +1 314 935 6091; fax: +1 314 935 4014.
E-mail address: rka@wustl.edu (R.K. Agarwal).

0378-7753/$ – see front matter © 2013 Elsevier B.V. All rights reserved.
http://dx.doi.org/10.1016/j.jpowsour.2013.09.011

The electric circuit based or equivalent circuit models (ECM) are the most intuitive for use in circuit simulations. These models are usually based on Thevenin equivalents and impedances. These models are simple and therefore are computationally less intensive. One of the main drawbacks of these models is their inability to predict the lifetime of the battery. However, their simplicity and the ability to predict the I–V characteristics make them suitable for dynamic modeling of the electric vehicles. An ECM comprises of a combination of resistances and capacitors. These parameters are multivariable functions of SOC, current, temperature, number of charge and discharge cycles etc. In order to use ECMs effectively in electric vehicle dynamic simulation, it is critical to determine the parameters of the circuit accurately; these parameters are usually determined by extensive experimentation [5]. In many situations the evaluation of the performance of an electric drive train may require experiments using different type of batteries from different manufacturers. These experiments are generally very resource intensive. Therefore it is generally not feasible to perform experiments for each type of battery to extract parameters for ECM. To overcome this problem, recently Kumar and Bauer [6] have suggested the application of a multi-objective genetic algorithm (MOGA) for extracting the battery parameters.

In this paper, we employ a modified version of the approach outlined in Ref. [6] for extracting the battery parameters and determine the charge and discharge characteristics of five batteries (three industry manufactured batteries and two batteries in research and development stage). The genetic algorithm holds greater benefits compared to other traditional parameter-estimation approaches when analytic solutions of the problem do not exist and when the number of design parameters are large which in this work are 31. The genetic algorithm is also well-known for its minimal requirements of prior knowledge of the solution-searching optimization problem. The computed results are compared with the catalog data (in case of industry manufactured batteries) and the experimental data (in case of batteries in research and development stage).

2. Methodology

Since the equivalent circuit model is described by a set of non-linear equations [5,6], it is not tractable for obtaining an analytical solution. However, the computations employing the solution searching technique can be used to determine the parameter values needed for modeling the batteries. Genetic algorithm (GA) appears to be an ideal candidate for such task. In this work, a modified version of multi-objective non-dominated sorting genetic algorithm (NSGA-II) has been employed [7]. The multi-objective genetic algorithm (MOGA) code was first validated by extracting the battery parameters for the battery [8] used in Ref. [6]; the results were compared with those obtained in Ref. [6]. After the validation, the battery modeling code was employed to extract the battery parameters of two additional industrial lithium-ion batteries [9,10] and the results were compared with the catalog data. Finally the code was applied to extract the optimal parameters of recently proposed high performance batteries, three Li–O_2 batteries [11] and two alkaline batteries with an iron electrode [12] and Potassium Hydroxide electrolyte; these two batteries are in early stage of research and development. For all the five cases, charging and discharging characteristics were obtained which were compared with either the catalog data (for industrial batteries) or with the experimental data (for research domain batteries).

2.1. Equivalent circuit battery model

The schematic of the equivalent circuit model (ECM) used in this work is shown in Fig. 1 [5,6]. The parameters in ECM are identified as the resistances (R_1, R_2), capacitance (C_1), and open circuit voltage of the battery (V_o). The presence of one pair of capacitance and resistance, i.e. C_1 and R_2, makes the model to be linear with time. However, non-linear ECM with more than one capacitance–resistance pairs has also been proposed [13,14], which is supposed to be more accurate in capturing the transient behavior of the battery. Non-linear ECM inevitably introduces more modeling parameters due to the increased model complexity. For simplicity, only the linear ECM shown in Fig. 1 is employed in this paper.

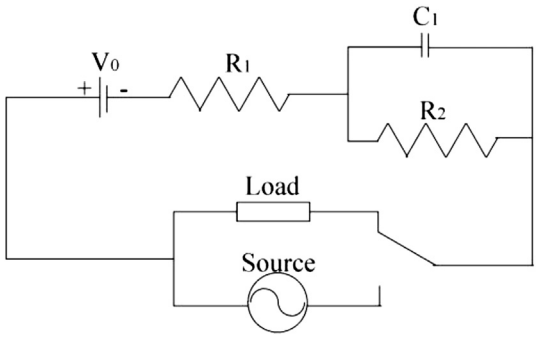

Fig. 1. Equivalent circuit model (ECM) of a battery [5,6].

These parameters are all functions of the current State-of-Charge (SOC) and discharge rate (C_r) of the battery, which can be formulated as following polynomials to account for nonlinear phenomenon in the battery [6]:

Resistance:

$$R_1 = \left(a_1 + a_2 C_r + a_3 C_r^2\right) e^{-a_7 \times \mathrm{SOC}} + \left(a_4 + a_5 C_r + a_6 C_r^2\right) \quad (1)$$

$$R_2 = \left(a_8 + a_9 C_r + a_{10} C_r^2\right) e^{-a_{14} \times \mathrm{SOC}} + \left(a_{11} + a_{12} C_r + a_{13} C_r^2\right) \quad (2)$$

Capacitance:

$$C_1 = -\left(a_{15} + a_{16} C_r + a_{17} C_r^2\right) e^{-a_{21} \times \mathrm{SOC}} + \left(a_{18} + a_{19} C_r + a_{20} C_r^2\right) \quad (3)$$

Open circuit voltage:

$$V_o = -\left(a_{22} + a_{30} C_r + a_{31} C_r^2\right) e^{-a_{23} \times \mathrm{SOC}} + \left(a_{24} + a_{25} \times \mathrm{SOC} + a_{26} \times \mathrm{SOC}^2 + a_{27} \times \mathrm{SOC}^3\right) - a_{28} C_r + a_{29} C_r^2 \quad (4)$$

In Equations (1)–(4), the coefficients a_1 through a_{31} are model parameters intrinsically determined by the battery and its operational condition, such as the operation temperature.

The time dependent voltage output of the battery cell is then given by the equation [15]:

$$V(t) = \frac{Q_o(0)}{C_1} e^{-t/R_2 C_r} + V_o - I R_1 - I R_2 \left(1 - e^{-t/R_2 C_r}\right) \quad (5)$$

where Q_0 is the nominal capacity of the battery cell (A h), t is time duration since charge/discharge starts (seconds), and I is the current (A).

Equations (1)–(5) describe the performance of a battery by $V(t)$ as a function of SOC, which varies from 0 to 100% of the battery's capacity. Nominal capacity Q_0 is the inherent property of a battery cell, thus it remains constant and can be measured. Charging/

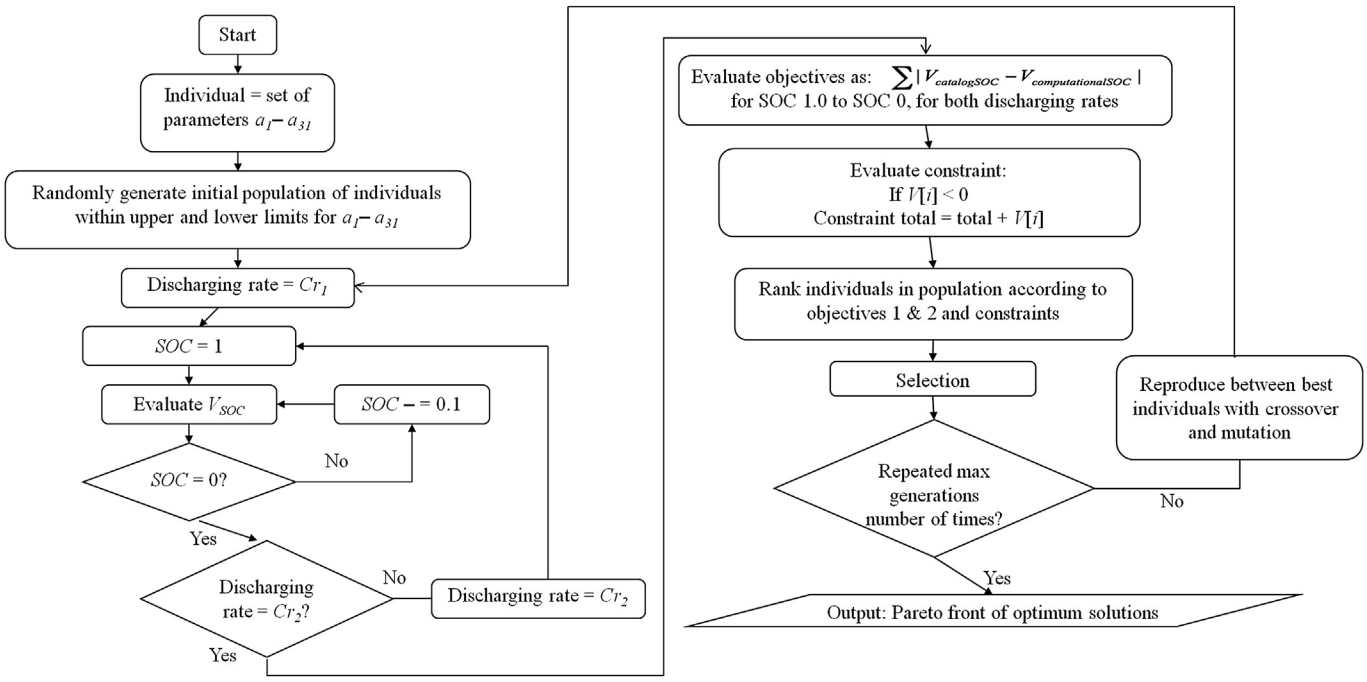

Fig. 2. Flowchart of the optimization process for determining a_1–a_{31} using the modified NSGA-II MOGA.

discharging rate C_r is controllable based on the demand of the application and is likely to remain constant for an identical operation. Therefore, in Equations (1)–(5) the model parameters, a_1–a_{31}, remain to be determined. Once the values of a_1–a_{31} are known, the complete battery model is established and its charging/discharging performance can be predicted by Equations (1)–(5). This model can then be employed in simulating the performance of an electric drive train.

3. The modified multi-objective NSGA-II genetic algorithm

Computer simulations of Equations (1)–(5) in conjunction with a multi-objective genetic algorithm (MOGA) provide an effective approach for extracting the battery parameters, a_1–a_{31}, for a particular battery. MOGA is used to find the values of these coefficients a_1–a_{31} that produce a voltage–SOC characteristic which best fits the experimentally measured curve by the battery manufacturer.

Multi-objective optimization problems require the optimization of multiple objectives. However, a single absolutely optimal solution satisfying multiple objectives cannot be achieved by employing MOGA. It can be accomplished by a genetic algorithm only for a single optimization objective. Instead, for a multi-objective problem a set of optimal solutions is obtained called the Pareto-front. The area which the Pareto-front covers is called the hyper-volume [16]. Any point inside the hyper-volume is considered to be dominated by at least one solution in the Pareto-front. However, the Pareto-front itself is non-dominated; meaning no one solution in this set can optimally satisfy all the objectives.

In this work, non-dominated sorting genetic algorithm (NSGA-II) is used [7]. The code based on NSGA-II is known as the j-metal code which can be obtained from the website [17]. The multi-objective genetic algorithm (MOGA) is a two-stage process. In this process, one set of parameters is considered to be one individual. First, a population of individuals is ranked by fitness and the best are selected to reproduce. Reproduction then takes place with mutation and cross-over to create an intermediate generation. The new generation is then ranked and the process repeats [18]. Mutation randomly occurs at low probabilities from one generation to the next, altering part of a particular individual. Reproduction is carried out through the random pairing of two individuals. Once matched, a random point on the pair is chosen where cross-over occurs and the two strings swap chunks of code [19]. The selection process is carried out by "binary tournaments". A population is divided into groups of a certain size. Each group competes in a tournament in which the individual with the highest fitness (lowest objective values) wins [20]. These winners are chosen as the parents for the next generation and the entire process is repeated.

To apply MOGA to our specific problem of battery parameter extraction, standard NSGA-II code [17] was modified. Sixteen sample points were read from the catalog voltage–SOC charging/discharging characteristics of a particular battery. Typically, two exponential regions (at high and low SOC) and one linear region (between high and low SOC) can be identified for most voltage–SOC characteristics. Therefore, it is best to have more sample points in the exponential regions to accurately capture the steep changes in the charging/discharging characteristics, and keeping fewer points for the linear region in order to save the computational resources.

Table 1
Batteries considered and the type of optimization applied to extract the battery parameters a_1–a_{31}.

Battery	Discharging	Charging
e-PLB [8]	M	M
Lithium-ion (ANR26650) [9]	M	S
Lithium-ion (Seiko MS614SE) [10]	M	S
Li–O_2 [11]	S	S
Li–O_2 (+composite carbon cathode) [11]	S	S
Li–O_2 (+gold loaded carbon cathode) [11]	S	S
Alkaline battery with iron electrode [12]	S	S
Alkaline battery with iron electrode with bismuth sulfide ADDITIVE) [12]	S	S

*S = single objective, M = multi-objective.

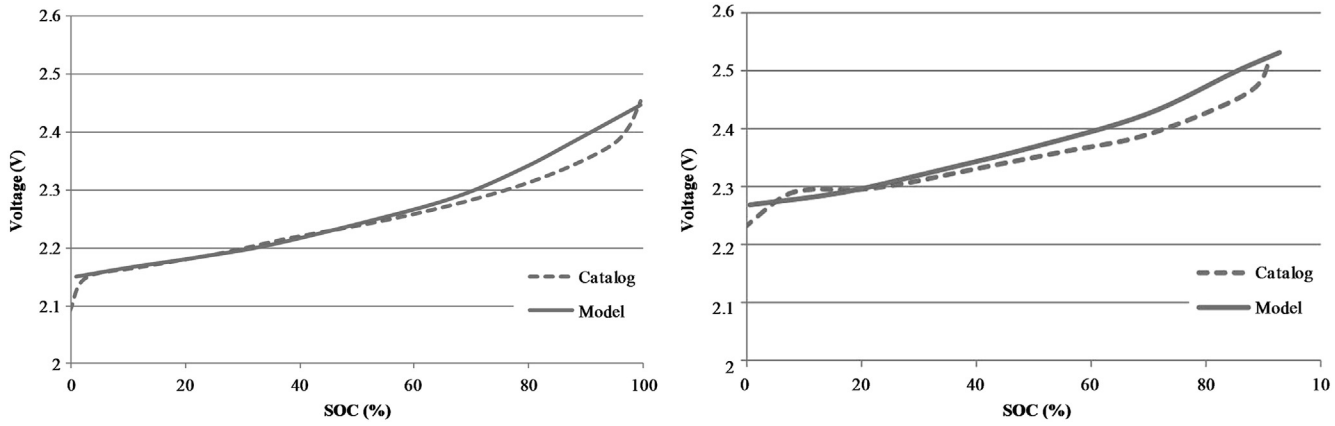

Fig. 3. Charging characteristics for C_r = 0.5 C (left) and 4 C (right) for ePLB battery.

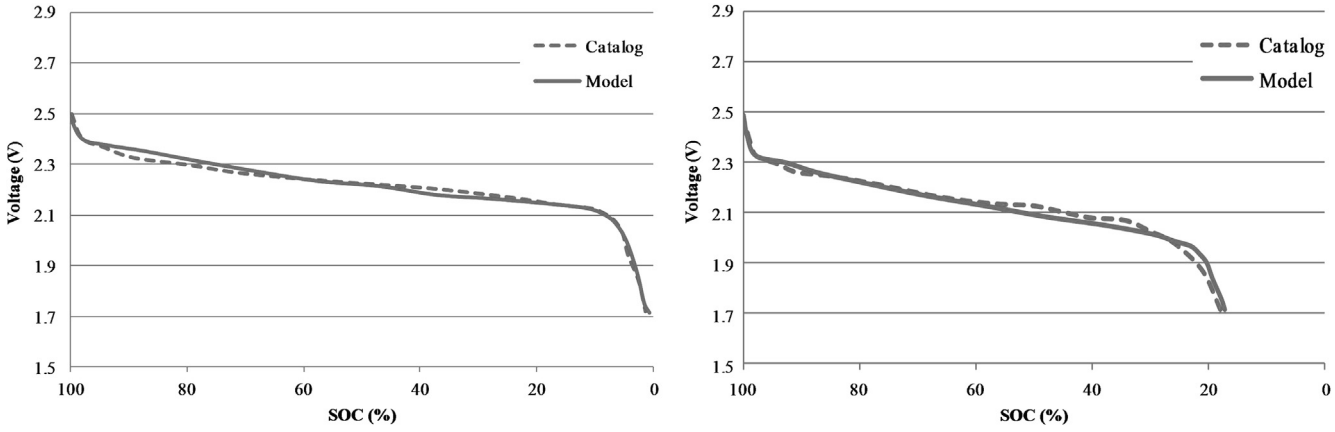

Fig. 4. Discharging characteristics for C_r = 0.5 C (left) and 4 C (right) for ePLB battery.

Since the ultimate goal is to determine the values a_1–a_{31} that would lead to minimum difference between the model output and the manufacturer provided battery characteristic curves, the objective function is defined as the absolute value of the difference between the model output and the catalog value at each sample point. The objective function is defined as:

$$\text{Objective}: f(x) = |V_c - V_g|_1 + |V_c - V_g|_2 + \ldots + |V_c - V_g|_n \tag{6}$$

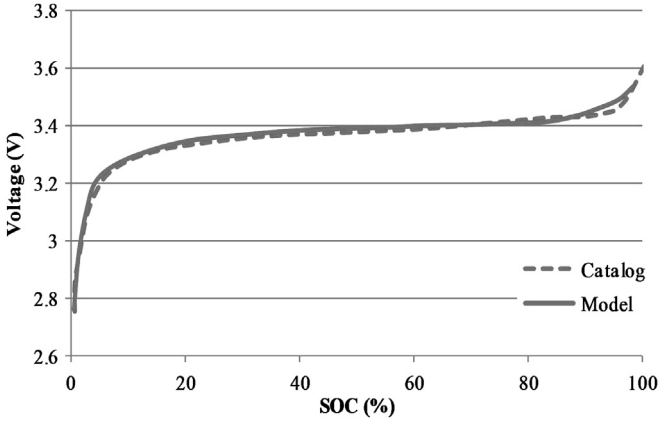

Fig. 5. Charging characteristics for C_r = 2 C.

where V_c is the catalog voltage value and V_g is the model output voltage value computed from the genetic algorithm by determining a_1–a_{31} at each generation; n is the number of sample points.

Equation (6) describes a single-objective optimization problem. However, recalling that the voltage characteristics are affected by the charging/discharging rate, a multi-objective optimization problem is formulated as follows:

Objectives 1–m are defined by the functions:

$$\begin{cases} f_1(x) = |V_c - V_g|_{1,Cr_1} + |V_c - V_g|_{2,Cr_1} + \ldots + |V_c - V_g|_{n,Cr_1} \\ f_2(x) = |V_c - V_g|_{1,Cr_2} + |V_c - V_g|_{2,Cr_2} + \ldots + |V_c - V_g|_{n,Cr_2} \\ \vdots \\ f_m(x) = |V_c - V_g|_{1,Cr_m} + |V_c - V_g|_{2,Cr_m} + \ldots + |V_c - V_g|_{n,Cr_m} \end{cases} \tag{7}$$

where m is the number of different charging/discharging rates.

The objective functions in Equation (7) are minimized by using MOGA. Closer to zero these functions become, better agreement is obtained between the catalog curve and the model output curve. Since negative voltage values are not expected, a constraint is implemented. For any set a_1–a_{31} which produces negative voltages, a constraint is implemented based on how many voltages are below zero and how negative the values of these voltages are. Individuals with no constraint are considered better fit than the individuals with a constraint. The MOGA simulation is considered converged when the desired minimum for the objectives in Equation (7) is achieved. The converged values of a_1–a_{31} provide the closest fit to the charging/discharging curve obtained by the battery model

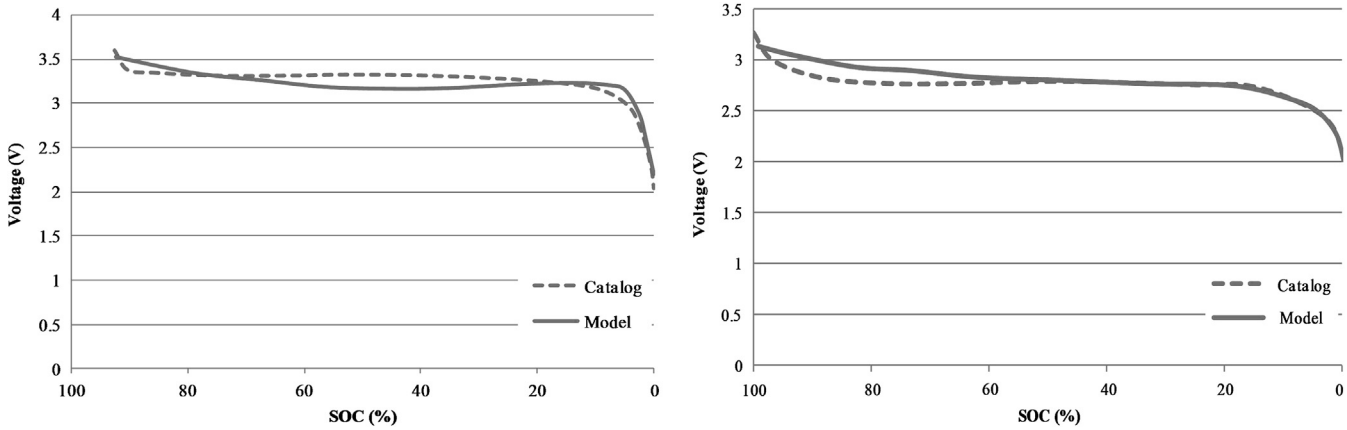

Fig. 6. Discharging characteristics for $C_r = 0.33$ C (left) and 10 C (right).

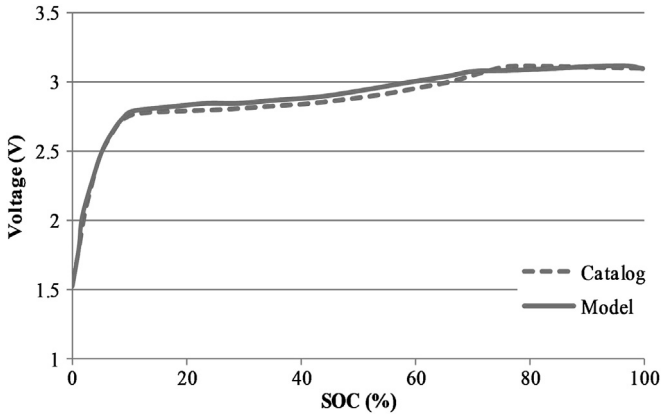

Fig. 7. Charging characteristics for $C_r = 6.7$ C.

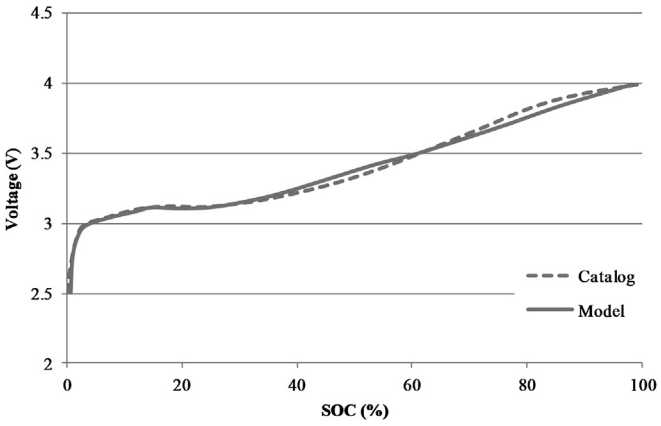

Fig. 9. Charging characteristics for 5000 mA g^{-1} current density.

given by Equations (1)–(5), when compared to the catalog curve. A flowchart explaining the entire optimization process for determining a_1–a_{31} is shown in Fig. 2.

4. Simulation results

In this paper, using MOGA, parameters are extracted for eight batteries, including three lithium-ion batteries (ePLB-cell [8], MS614SE-cell [9], and ANR26650M1-cell [10]), three Li–O_2 batteries [11], and two alkaline batteries with iron electrode [12]. Based on the data availability of battery characteristics under different charging/discharging rates, either a single-objective optimization or a multi-objective optimization was applied. A list of batteries considered and the type of optimization employed is given in Table 1.

4.1. Battery #1: ePLB cell [8]

The ePLB-cell [8] was modeled using ECM and MOGA in Ref. [1]; this case has been used for our code validation using ECM and

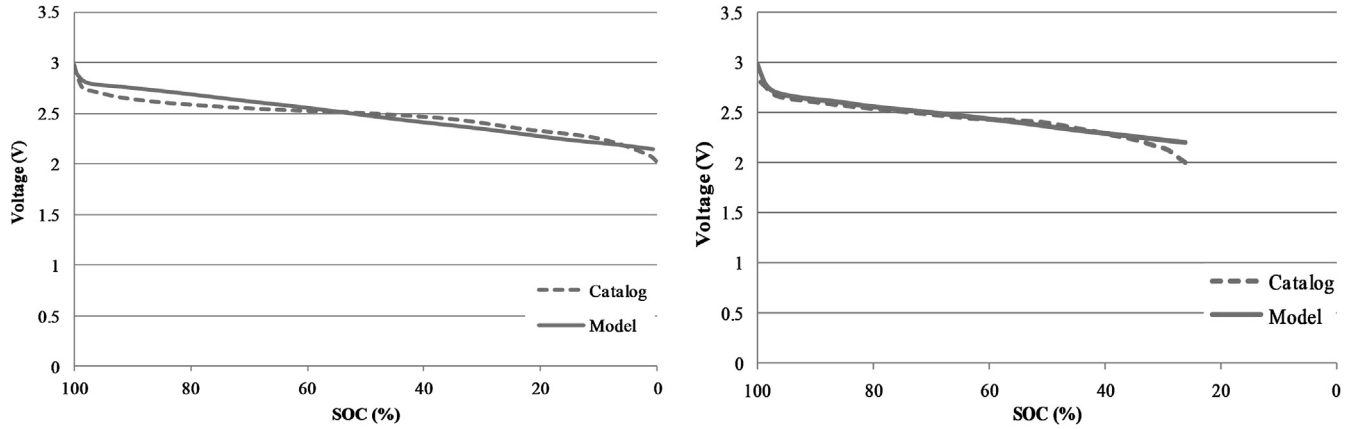

Fig. 8. Discharging characteristics for $C_r = 1$ C (left) and 6.7 C (right).

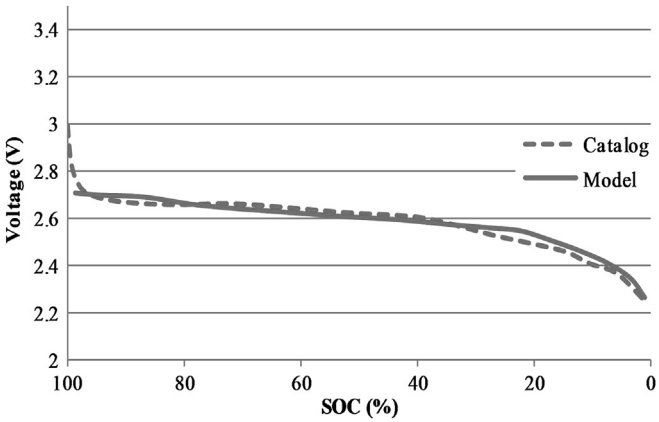

Fig. 10. Discharging characteristics for 5000 mA g^{-1} current density.

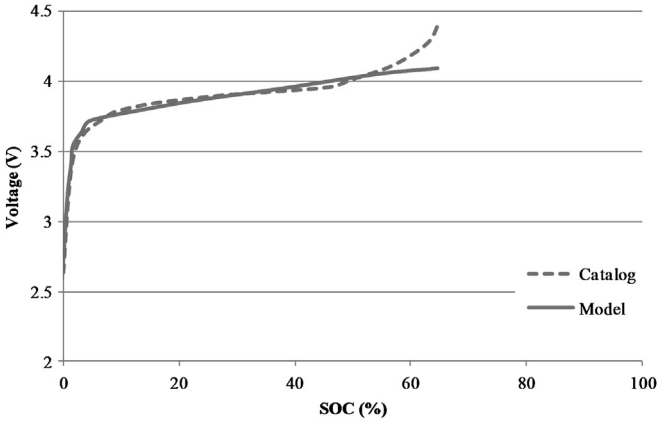

Fig. 11. Charging characteristics for 70 mA g^{-1} current density.

MOGA. Two charging and discharging rates of C_r = 0.5 C and 4 C (C = 8 A) were considered. The extracted battery parameters a_1–a_{31} are summarized in the appendices in Table A1. The computed charging and discharging characteristics and their comparisons with catalog data are shown in Figs. 3 and 4 respectively.

4.2. Battery #2: ANR26650 cell [9]

ANR26650 battery is the next generation of A123 Systems pioneering 26650 cylindrical cells. It is a high power battery cell with large energy density and lower impedance. Due to its versatility, the ANR26650 battery is used in a wide variety of applications e.g. in EVs and HEVs. Fig. 5 shows the comparison of our model's output with catalog data [9] for charging characteristics for C_r = 2 C (C = 3 A) and Fig. 6 shows the comparison of our model's output with catalog data [9] for discharging characteristics for C_r of 0.33 C and 10 C (C = 3 A). Table A1 in appendices summarizes the extracted parameters a_1–a_{31} for this battery.

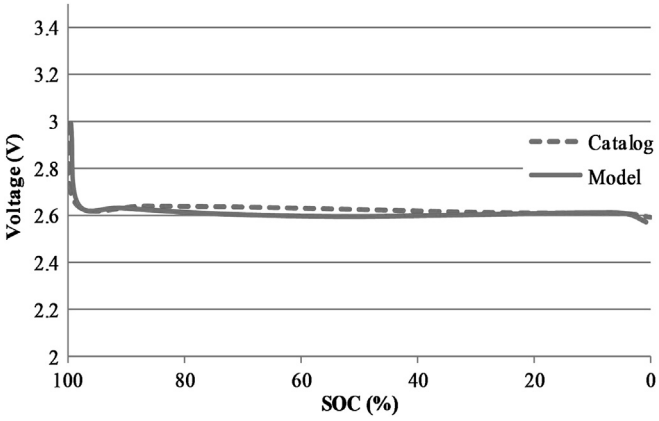

Fig. 12. Discharging characteristics for 70 mA g^{-1} current density.

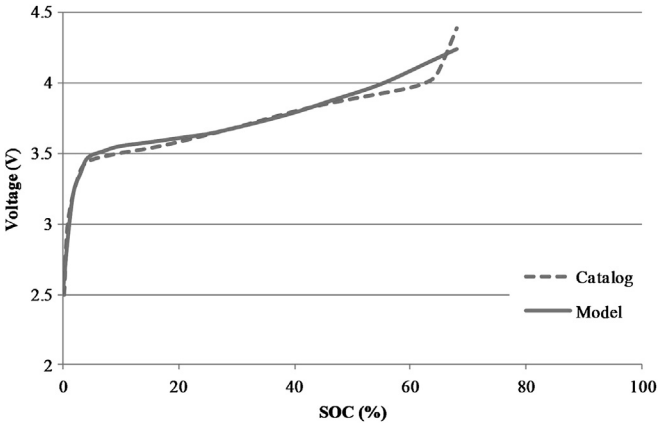

Fig. 13. Charging characteristics for 70 mA g^{-1} current density.

4.3. Battery #3: MS614SE cell [10]

MS614SE cell is a high-performance rechargeable micro battery produced by Seiko Instruments for sophisticated electronic instruments and equipment. Fig. 7 shows the comparison of our model's output with catalog data [10] for charging characteristics for C_r = 6.7 C (C = 15 μA) and Fig. 8 shows the comparison of our model's output with catalog data [10] for discharging characteristics for C_r of 1 C and 6.7 C (C = 15 μA). Table A1 in appendices summarizes the extracted parameters a_1–a_{31} for this battery.

4.4. Battery #4: Li–O_2 cell [11]

In a recent research paper, rechargeable non-aqueous Li–O_2 battery has been proposed [11]; it is receiving a great deal of interest because of its high specific energy which far exceeds the best achievable by lithium-ion cells. Fig. 9 shows the comparison of our model's output with the experimental data [11] for charging characteristics under 5000 mA g^{-1} charging current density

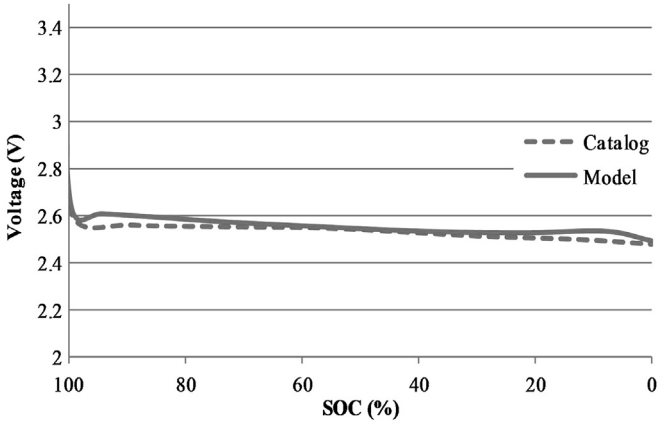

Fig. 14. Discharging characteristics for 70 mA g^{-1} current density.

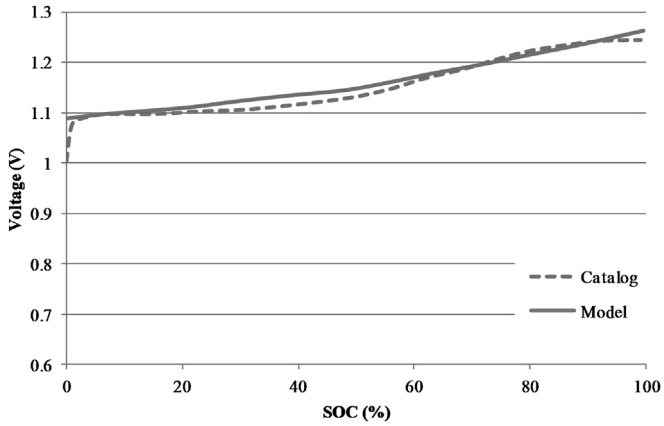

Fig. 15. Charging characteristics for $C_r = 0.5$ C.

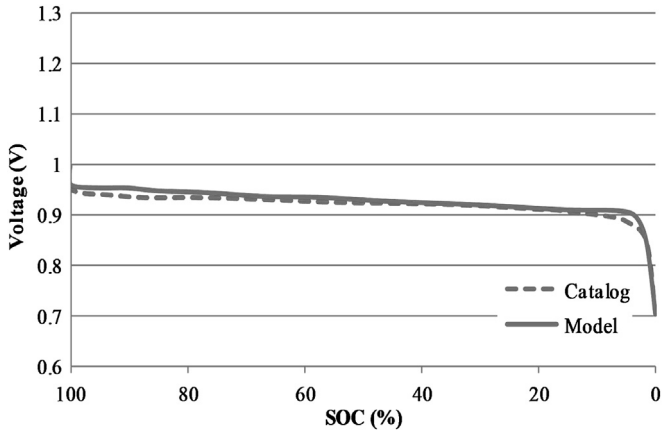

Fig. 16. Discharging characteristics for $C_r = 0.05$ C.

(normalized by the mass of carbon) and Fig. 10 shows the comparison of our model's output with data [11] for discharging characteristics under 5000 mA g^{-1} discharging current density (normalized by the mass of carbon). The extracted battery parameters a_1–a_{31} are summarized in the appendices in Table A1.

4.5. Battery #5: Li–O_2 cell (with composite carbon cathode) [11]

Figs. 11 and 12 show the comparison of our model's output with the experimental data [11] for charging and discharging characteristics under 70 mA g^{-1} current density (normalized by the mass of carbon) respectively. The extracted battery parameters a_1–a_{31} are summarized in the appendices in Table A1.

4.6. Battery #6: Li–O_2 cell (with gold loaded composite carbon cathode) [11]

Figs. 13 and 14 show the comparison of our model's output with the experimental data [11] for charging and discharging characteristics under 70 mA g^{-1} current density (normalized by the mass of carbon) respectively. The extracted battery parameters a_1–a_{31} are summarized in the appendices in Table A1.

4.7. Battery #7: alkaline battery with iron electrode and KOH electrolyte cell [12]

Recently, iron-based alkaline batteries have been identified as a potential solution in addressing the challenges of durability, cost,

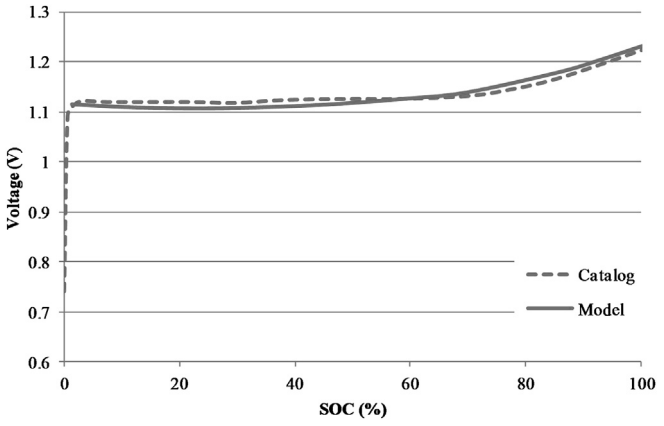

Fig. 17. Charging characteristics for $C_r = 0.5$ C.

and large-scale implementation of energy storage. Batteries with carbonyl iron electrodes have been studied in Ref. [12] where their charging and discharging characteristics have been reported. Fig. 15 shows the comparison of our model's output with the experimental data [12] for charging characteristics for $C_r = 0.5$ C ($C = 0.36$ A) and Fig. 16 shows the comparison of our model's output with data [12] for discharging characteristics for $C_r = 0.05$ C ($C = 0.36$ A). The extracted battery parameters a_1–a_{31} are summarized in Table A1.

4.8. Battery #8: alkaline battery with iron electrode with bismuth sulfide and KOH electrolyte cell [12]

To improve the specific capacity and charging efficiency of iron batteries, bismuth sulfide can be added [12]. Figs. 17 and 18 show the comparison of our model's output with the experimental data [12] for charging characteristics for $C_r = 0.5$ C ($C = 0.64$ A) and discharging characteristics for $C_r = 0.05$ C ($C = 0.64$ A) respectively. The extracted battery parameters a_1–a_{31} are summarized in Table A1.

5. Conclusions

In this work, a modified NSGA-II multi-objective genetic algorithm [7] based optimization code has been developed to effectively perform the extraction of battery parameters required for modeling the charging/discharging performance of a battery using an equivalent circuit model for application in electric drive train simulation of electric vehicles. The results obtained from our code for eight different batteries are in reasonably good agreement with

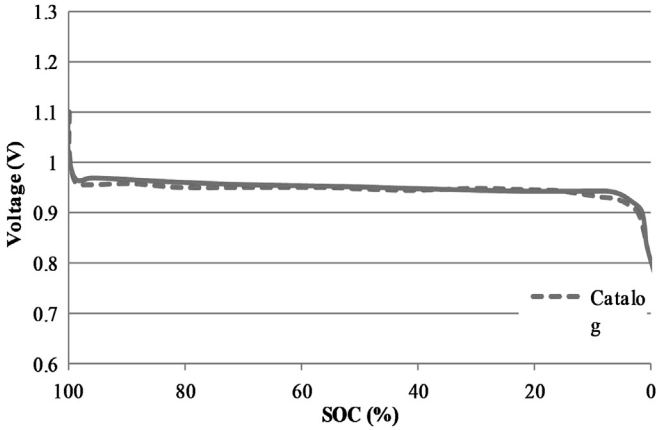

Fig. 18. Discharging characteristics for $C_r = 0.05$ C.

the catalog/experimental data for charging/discharging characteristics. The results suggest that the developed code can be used with confidence for extraction of battery parameters needed in an ECM model for a large variety of batteries with different sizes, capacities, materials, etc. It should however be noted that the model outputs of charging/discharging characteristics from our code may slightly differ from the catalog characteristics in some cases, especially at low and high SOC when drastic changes in voltage may occur. This suggests future improvement in the code may include weighting of the point distribution in these regions.

Appendices

Table A1
Battery parameters a_1–a_{31} for various batteries under consideration

	Validation		ANR26650	Seiko MS614SE	Li–O_2	
	Discharging	Charging	Discharging	Discharging	Discharging	Charging
a_1	0.20835291	0.30689735	0.00461877	0.091205243	0.01073646	53.5953143
a_2	0.03579959	0.01562162	4.8659E-06	0.540474998	0.18975732	1.42771541
a_3	0.00039606	0.00685809	0.01179723	0.820580154	0.78228093	10.5988734
a_4	0.15919108	0.10903136	0.7512944	0.118955849	0.17712076	0.05123828
a_5	0.0058729	0.01125884	0.07957936	0.946536	0.97380714	0.16838811
a_6	0.014583	0.0124507	0.017111	0.803583273	0.57579603	0.53580137
a_7	0.84904339	0.13708388	0.37531505	0.773938703	0.96127054	19.7204805
a_8	0.01799999	5.51E-05	0.89502179	8.628790134	4.57E-05	0.00460395
a_9	0.07685504	1.38E-05	0.45275245	1.691575926	0.29136878	0.62259064
a_{10}	0.4562723	5.10E-06	0.93659989	0.674445879	0.01467387	0.02035467
a_{11}	3.9482E-05	1.92E-05	0.00071951	0.036847234	8.99E-06	0.14779553
a_{12}	6.3776E-07	1.68E-05	0.0013407	0.994080133	1.51E-05	0.79662184
a_{13}	2.2766E-06	3.47E-06	0.03375708	0.918395111	3.14E-06	0.95324255
a_{14}	38.8827613	0.92172096	45.9334064	17.14106692	12.2351843	69.9632914
a_{15}	0.01402422	0.45025886	1.03289541	−70.2324694	0.43140728	0.31602659
a_{16}	0.13564355	0.37415859	9.67102855	−68.40602547	0.53229058	0.59819497
a_{17}	0.01853951	0.03503156	7.67531457	7.37606324	0.32551931	0.14692834
a_{18}	9.92993734	0.90074554	9.96331567	16.54940513	9.18060086	4.14873414
a_{19}	9.708302	0.83842829	6.62020206	1.424637761	9.92182253	2.92392616
a_{20}	8.79748508	0.9166211	9.91798063	21.5736066	9.76708248	7.15771813
a_{21}	0.67106684	0.5192527	3.39887702	7.91293592	0.23486365	0.29390599
a_{22}	1.69655185	0.03956599	2.18565757	1.249609558	0.50907584	2.38881108
a_{23}	0.52269596	0.12123495	0.297832	0.160405955	0.60452313	0.19900778
a_{24}	1.69347882	3.57513804	1.42529313	0.926040945	1.97255537	1.90399394
a_{25}	0.27104638	0.01323247	0.34651381	0.86168063	0.66879075	2.13001815
a_{26}	0.13853725	3.73E-05	0.01210208	0.000793251	8.34E-04	4.37E-04
a_{27}	0.33570299	0.17322835	0.54727467	1.91075E-05	0.02384203	0.00190092
a_{28}	0.86261017	0.61028401	0.17518266	5.272873439	0.15386122	0.78542756
a_{29}	0.73759611	0.72975429	0.6578156	0.876496134	0.34071846	0.11985901
a_{30}	0.81575463	0.34930874	0.75252781	0.10467427	0.80860882	0.80790961
a_{31}	0.71762382	0.9163944	0.47158002	0.873173876	0.34129681	0.38748586

	Li–O_2 carbon		Li–O_2 gold loaded		Iron		Iron + bismuth sulfide	
	Discharging	Charging	Discharging	Charging	Discharging	Charging	Discharging	Charging
a_1	0.82432906	14.5241027	0.26549751	14.1224938	29.4914986	0.45462307	14.5599838	0.55333126
a_2	0.16163508	24.4756143	0.66016791	4.40953222	72.9081168	0.54913924	11.1430598	0.9640732
a_3	0.99902869	2.63245697	0.93141066	37.0450311	73.0177209	0.12070674	38.1558624	0.40420978
a_4	0.79862881	0.25224944	0.27658709	0.00590928	0.26222204	0.75297676	0.25523467	0.54544581
a_5	0.64920124	0.1630204	0.15746281	0.3036228	0.09864263	0.98736132	0.81490269	1.95806029
a_6	0.41082605	0.00278872	0.49241206	0.56180101	0.78515787	0.11234894	0.61007881	0.73571603
a_7	0.53770096	119.108559	0.48588926	75.4897042	149.996207	0.30099129	88.931616	0.17610559
a_8	0.99676323	0.99948113	0.61531353	0.00317614	0.08526336	8.61E-11	0.85858184	1.08E-10
a_9	0.98328136	0.99956374	0.46278238	0.28678398	0.25717061	1.09E-07	0.06270029	2.76E-10
a_{10}	0.86287458	0.93117929	0.21019478	0.0982417	0.646143	4.69E-06	0.87188255	6.66E-08
a_{11}	1.93E-05	0.02263178	5.46E-06	0.0382265	5.60E-05	3.33E-07	8.11E-08	1.12E-09
a_{12}	4.35E-04	0.4718394	5.23E-05	0.31200386	3.20E-04	3.08E-08	0.00160551	6.40E-09
a_{13}	0.00321498	0.08762695	0.00705363	0.30672593	0.02603126	4.01E-10	0.02568106	2.39E-09
a_{14}	15.019207	13.3261146	14.8134438	144.115905	149.983968	0.4571012	149.852995	0.06898583
a_{15}	0.07644745	0.09699596	0.04481933	0.60145006	3.41E-06	0.06429345	0.02258402	0.00345412
a_{16}	0.33011917	0.94621908	0.29095625	0.44992672	0.04565322	0.25185158	0.01134694	0.00376443
a_{17}	0.28219357	0.31727155	0.62979428	0.50843293	0.09046255	0.39543831	0.29202957	0.23512432
a_{18}	9.88748962	0.00364755	9.54738307	0.19036418	9.99996127	0.92995916	9.90334007	8.71964227
a_{19}	9.99319013	0.82662482	9.05491208	3.52250087	9.97043314	0.83240631	8.35353122	7.96101789
a_{20}	8.42971362	7.16279946	9.88223081	9.60579147	7.92405725	0.9479404	7.82615417	8.82767317
a_{21}	0.48624695	0.17460783	0.93659762	0.06051375	0.85690665	0.8306388	0.20653592	0.65028507
a_{22}	1.29634101	1.20141209	1.5572842	2.76280474	0.63327953	0.08588711	0.02121622	0.50355483
a_{23}	0.20261211	1.40E-04	0.10064423	0.66444894	0.23745515	0.26704514	0.14166353	0.16544309
a_{24}	1.46582257	2.57245923	1.00973436	0.85216059	0.29576144	2.37981823	0.93034068	0.39883709
a_{25}	0.00295324	0.5439663	0.09635125	2.10345909	0.19194707	0.009514	0.01259381	0.10754302
a_{26}	0.19549466	1.69E-04	0.11227219	0.33182808	6.31E-07	0.1029671	0.01995769	0.00102557

Table A1 (*continued*)

	Li–O_2 carbon		Li–O_2 gold loaded		Iron		Iron + bismuth sulfide	
	Discharging	Charging	Discharging	Charging	Discharging	Charging	Discharging	Charging
a_{27}	0.02204306	3.47E-04	3.84E-04	0.5021228	2.74E-07	0.00852127	0.0052646	0.14710023
a_{28}	0.29079774	0.81658536	0.83635088	0.82468851	0.9616469	0.35565489	0.54176887	0.27629373
a_{29}	0.88948186	0.84944614	0.04848865	0.507183	0.4414678	0.0153644	0.16401757	0.81392545
a_{30}	0.26938344	0.64625688	0.91331299	0.05154254	0.48510127	0.52007456	0.36083715	0.65849334
a_{31}	0.05713941	0.35704537	0.83708787	0.00115925	0.44912057	0.25172147	0.19398491	0.96059927

References

[1] J. Larmine, J. Lowry, Electric Vehicle Technology Explained, first ed., John Wiley & Sons, 2003.
[2] North American Reliability Corporation, Accommodating High Levels of Variable Power Generation, April 2009 (accessed 12.06.13), http://www.nerc.com/files/IVGTF_Report_041609.pdf.
[3] Y.V. Makarov, J.G. Yang, S. DeSteese, S. Lu, C.H. Miller, P. Nyeng, J. Ma, D.J. Hammerstorm, V.V. Viswanathan, Wide Area Energy Storage and Management System to Balance Intermittent Resources in the Bonneville Power Administration in California ISO Control Areas, Pacific Northwest National Laboratory, June 2008. PNNL-17574.
[4] O. Tremblay, L.A. Dessaint, A.I. Dekkich, in: Proceeding of: Vehicle Power and Propulsion Conference, 2007, pp. 284–289.
[5] Y. Bor, G. Liaw, R. Nagasubramanian, G. Jungst, D.H. Doughty, J. Solid State Ionics 175 (2004) 835–839.
[6] P. Kumar, P. Bauer, in: Proceeding of: International Power Electronics and Motion Control Conference, 2010, pp. 106–110.
[7] K. Deb, A. Pratap, S. Agarwal, T. Meyarivan, IEEE Trans. Evol. Comput. 6 (2) (2002) 182–197.
[8] Energy Innovation Group, www.eigbattery.com (accessed 12.06.13).
[9] ANR26650 product catalog, A123 Systems, http://www.a123systems.com/lithium-ion-cells-26650-cylindrical-cell.htm (accessed 12.06.13).
[10] MS614SE product catalog, Seiko Instruments Inc., http://www.sii.co.jp/components/battery/productSpecBatEN.jsp?recordID=74 (accessed 12.06.13).
[11] Z. Peng, S.A. Freunberger, Y. Chen, P.G. Bruce, Sci. Express 337 (6094) (2012) 563–566.
[12] A.K. Manohar, S. Malkhandi, B. Yang, C. Yang, G.K. Surya Prakash, S.R. Narayanan, J. Electrochem. Soc. 159 (8) (2012) A1209–A1214.
[13] M. Chen, G.A. Rincon-Mora, IEEE Trans. Energy Convers. 21 (2) (2006) 504–511.
[14] K.S. Hariharan, V.S. Kumar, J. Power Sources 222 (15) (2013) 210–217.
[15] M.W. Verbrugge, R.S. Conell, J. Electrochem. Soc. 149 (2002) A45–A53.
[16] J.M. Bader, Hyper-volume Based Search for Multi-objective Optimization: Theory and Methods, CreateSpace Independent Publishing Platform, 2010.
[17] A Framework for Multi-objective Optimization, http://jmetal.sourceforge.net (accessed 12.06.13).
[18] J.J. Durillo, A.J. Nebro, C.A. Coello, J. Garcia-Nieto, F. Luna, E. Alba, IEEE Trans. Evol. Comput. 14 (4) (2010) 618–635.
[19] D. Whitley, A Genetic Algorithm Tutorial, Colorado State University, http://reference.kfupm.edu.sa/content/g/e/a_genetic_algorithm_tutorial_80073.pdf (accessed 12.06.13).
[20] B.L. Miller, D.E. Goldberg, Complex Syst. 9 (1995) 193–212.